Electronic Supplementary Material (ESI) for Inorganic Chemistry Frontiers.

Electronic Supplementary Information

Magnetic mesoporous TiO_2 microspheres for sustainable arsenate removal from acidic environment

Yujuan Zhao,[a] Changyao Wang,[a] Shuai Wang,[a] Chun Wang,[a] Yupu Liu,[a] Areej Abdulkareem Al-Khalaf,[b] Wael N. Hozzein,[c,d] Linlin Duan,[a] Wei Li*[a] and Dongyuan Zhao*[a]

[a] Department of Chemistry, Laboratory of Advanced Materials, Shanghai Key Lab of Molecular Catalysis and Innovative Materials, *i*ChEM and State Key Laboratory of Molecular Engineering of Polymers, Fudan University, Shanghai 200433, P. R. China.

[b] Biology Department, College of Sciences, Princess Nourah Bint Abdulrahman University, Riyadh, Saudi Arabia

[c] Bioproducts Research Chair, Zoology Department, College of Science, King Saud University, Riyadh 11451, Saudi Arabia

[d] Botany and Microbiology Department, Faculty of Science, Beni-Suef University, Beni-Suef, Egypt.

E-mail: dyzhao@fudan.edu.cn, weilichem@fudan.edu.cn

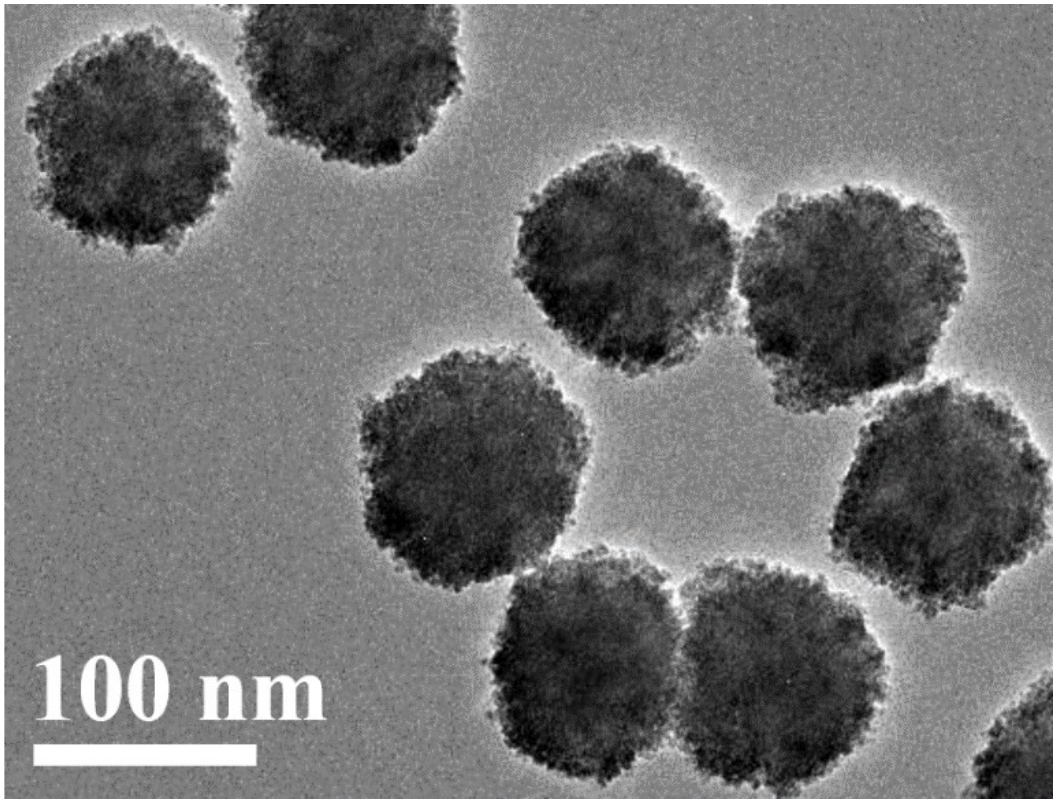

Fig. S1 The TEM image of the magnetite Fe_3O_4 nanoparticles prepared by a modified solvothermal reaction by aging a glycol solution of $FeCl_3 \cdot 6H_2O$ (3.25 g), trisodium citrate (1.3 g), and sodium acetate (6.0 g) at 200 °C for 10 h.

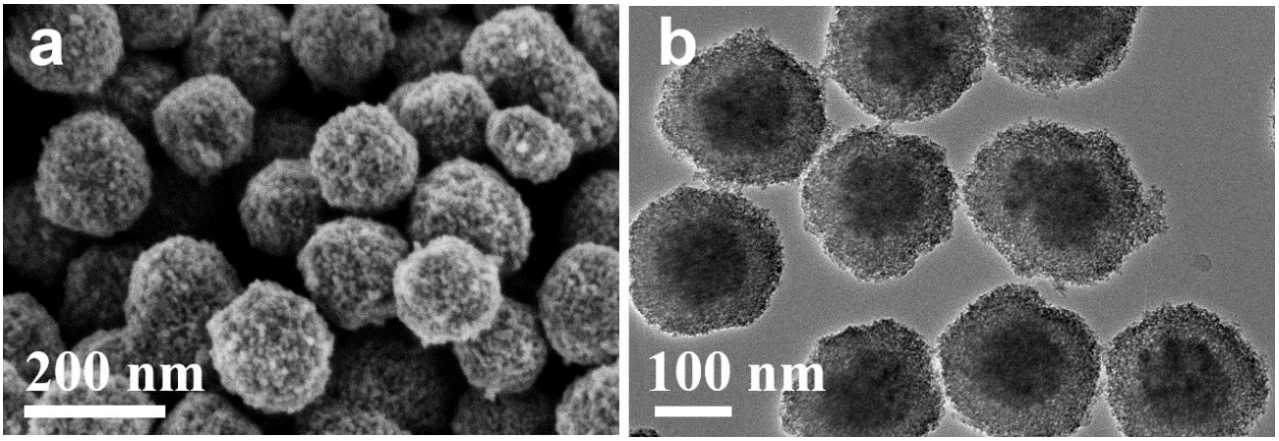

Fig. S2 SEM (a) and TEM (b) images of the core-shell structured Fe_3O_4@mTiO_2 microspheres prepared through the versatile kinetics-controlled coating method followed by calcining at 200 °C for 3 h in air.

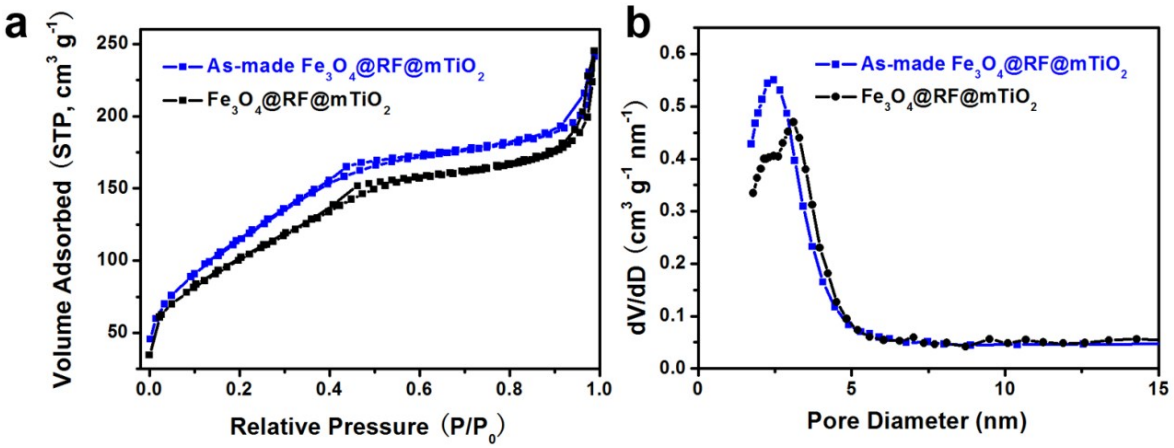

Fig. S3 The nitrogen adsorption/desorption isotherms (a) and the corresponding pore size distribution curves (b) of the as-made Fe_3O_4@RF@$mTiO_2$ and calcined Fe_3O_4@RF@$mTiO_2$ microspheres. The as-made Fe_3O_4@RF@$mTiO_2$ microspheres were obtained by the successive sol–gel coating method and the versatile kinetics-controlled coating method. The Fe_3O_4@RF@$mTiO_2$ microspheres were fabricated by calcining the as-made Fe_3O_4@RF@$mTiO_2$ microspheres at 200 °C for 3 h in air.

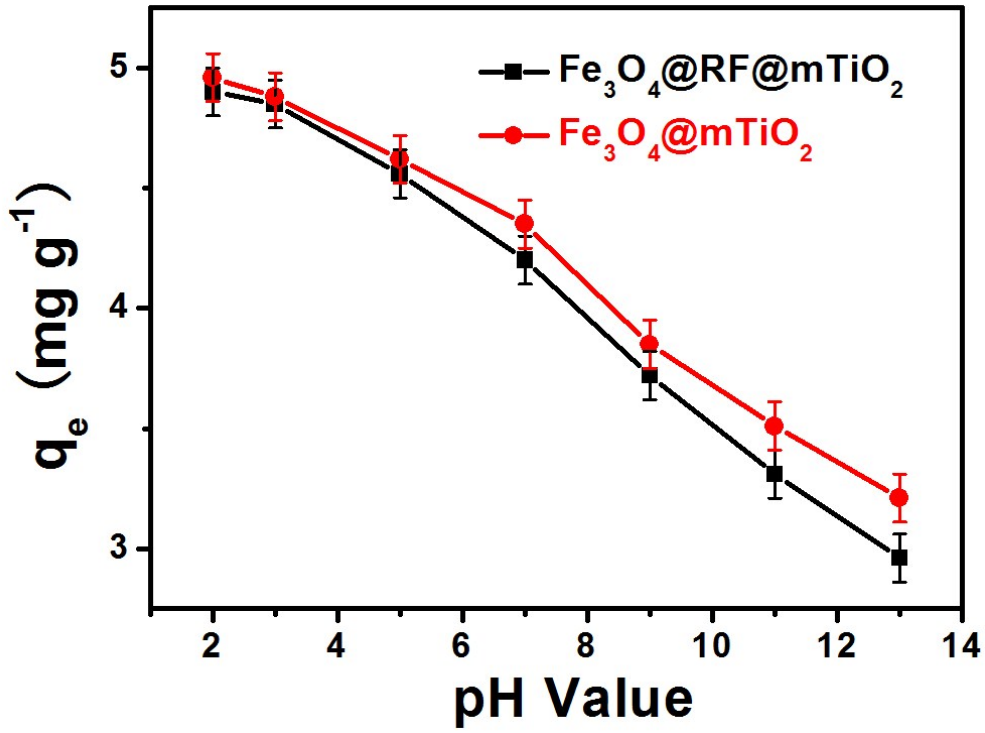

Fig. S4 The influence of pH values on As^{V} adsorption for the core-shell structured Fe_3O_4@RF@$mTiO_2$ and Fe_3O_4@$mTiO_2$ microspheres. The adsorption amounts of Fe_3O_4@RF@$mTiO_2$ and Fe_3O_4@$mTiO_2$ nano-adsorbents decreased with the increase of the pH values. The Fe_3O_4@RF@$mTiO_2$ and Fe_3O_4@$mTiO_2$ microspheres were fabricated by calcining the corresponding as-made Fe_3O_4@RF@$mTiO_2$ and as-made Fe_3O_4@$mTiO_2$ microspheres at 200 °C for 3 h in air, respectively.

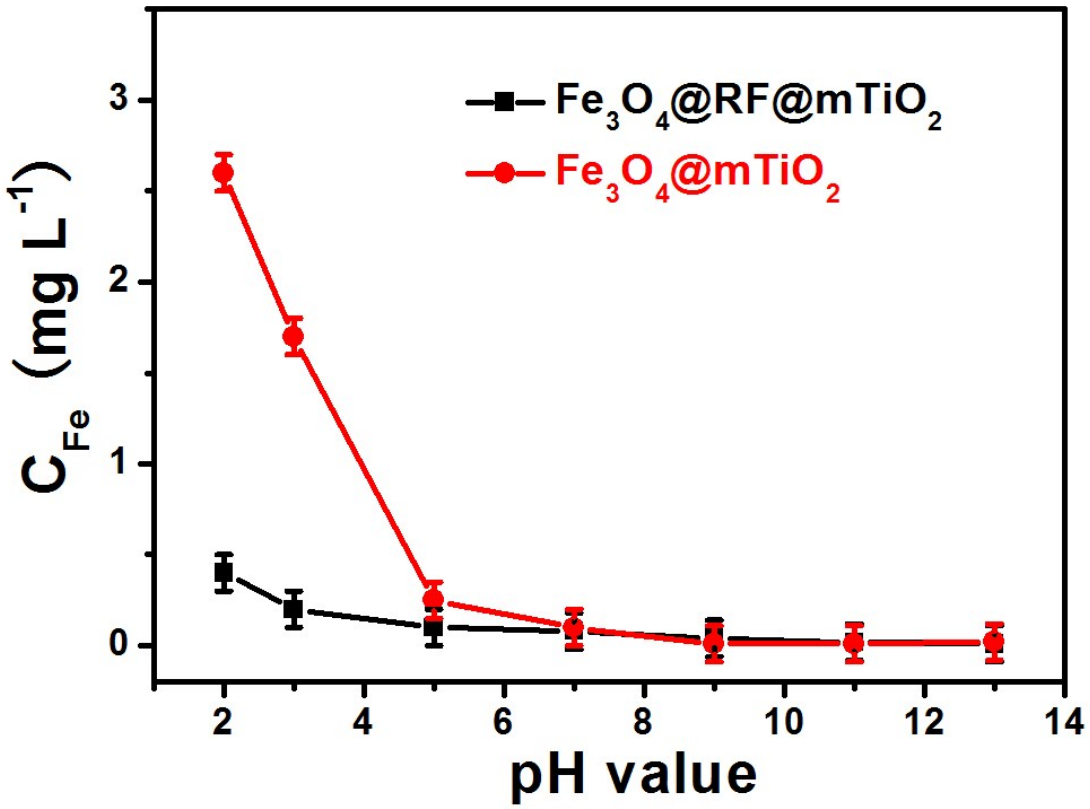

Fig. S5 The concentration of iron ions in the residual solution after As^{V} adsorption by the Fe_3O_4@RF@$mTiO_2$ and Fe_3O_4@$mTiO_2$ microspheres within different pH values (the initial arsenate concentration was 5 mg·L^{-1}). The Fe_3O_4@RF@$mTiO_2$ and Fe_3O_4@$mTiO_2$ microspheres were fabricated by calcining the corresponding as-made Fe_3O_4@RF@$mTiO_2$ and as-made Fe_3O_4@$mTiO_2$ microspheres at 200 °C for 3 h in air, respectively.

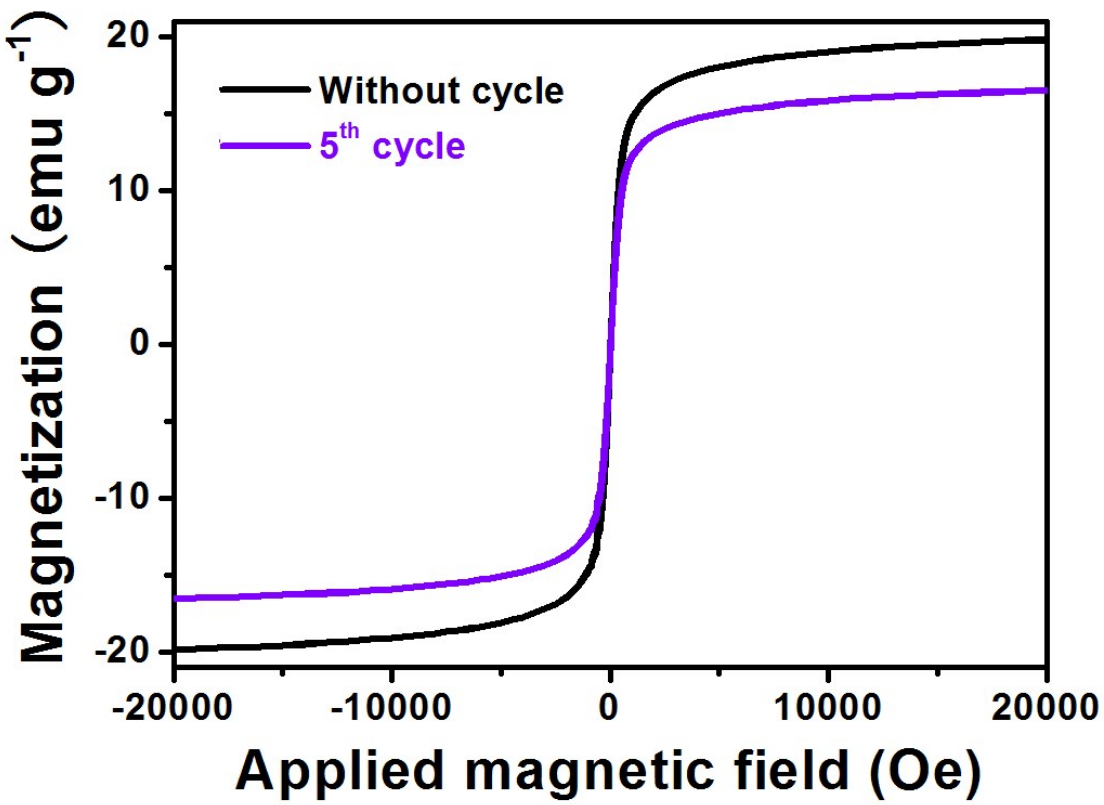

Fig. S6 The magnetic hysteresis loops of the multilayer core-shell structured Fe_3O_4@RF@mTiO_2 microspheres before As^V adsorption and after five As^V adsorption cycles.

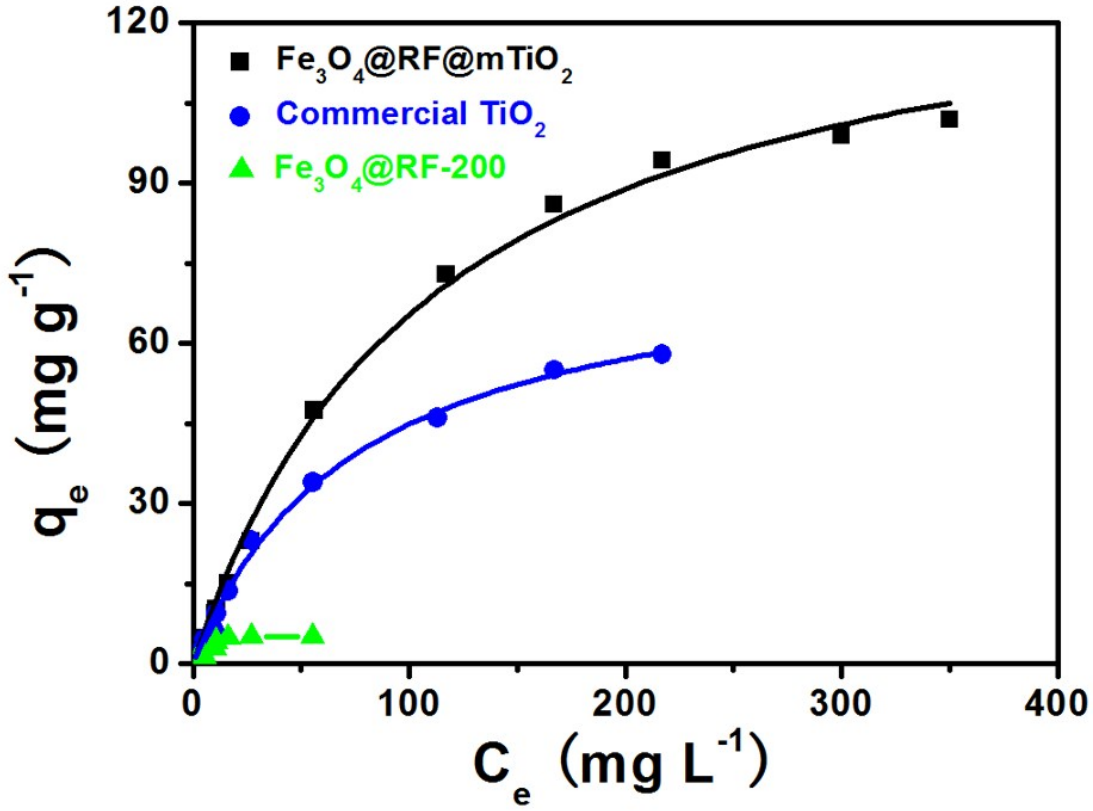

Fig. S7 Adsorption isotherms of As^V on the multilayer core-shell Fe_3O_4@RF@mTiO_2 microspheres, commercial TiO_2, and Fe_3O_4@RF-200 microspheres at 25 °C, suggesting the better As^V adsorption performance than the commercial TiO_2 and Fe_3O_4@RF-200 microspheres. Typically, 20 mg of adsorbents were dissolved into 20 mL of As^V solution with different concentrations (1–350 mg·L^{-1}). The Fe_3O_4@RF-200 microspheres were produced by calcining the Fe_3O_4@RF microspheres at 200 °C in air for 3 h.

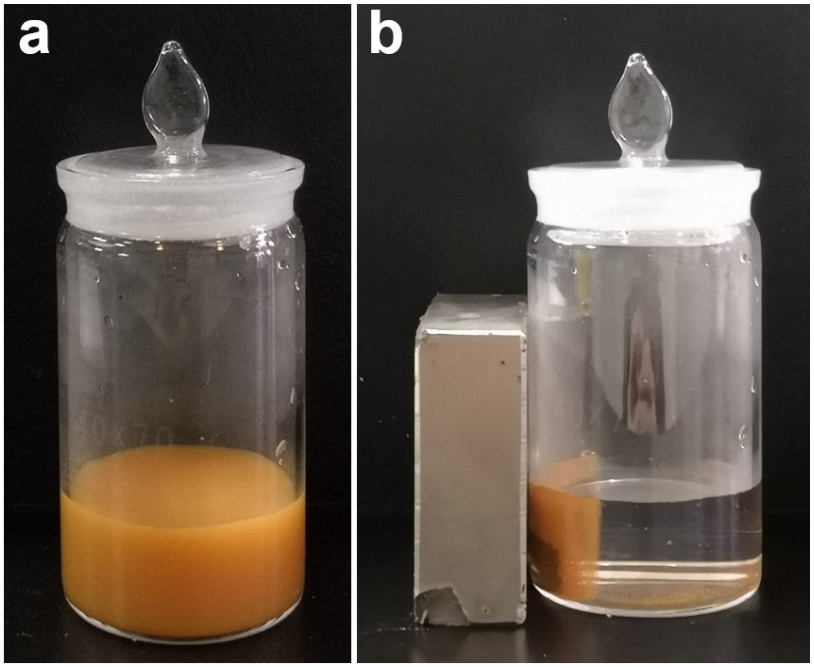

Fig. S8 The optical photos of (a) 20 mg of the Fe_3O_4@RF@mTiO_2 microspheres dispersed in 20 mL of deionized water by ultrasound and (b) separated by a magnet after 10 minutes.

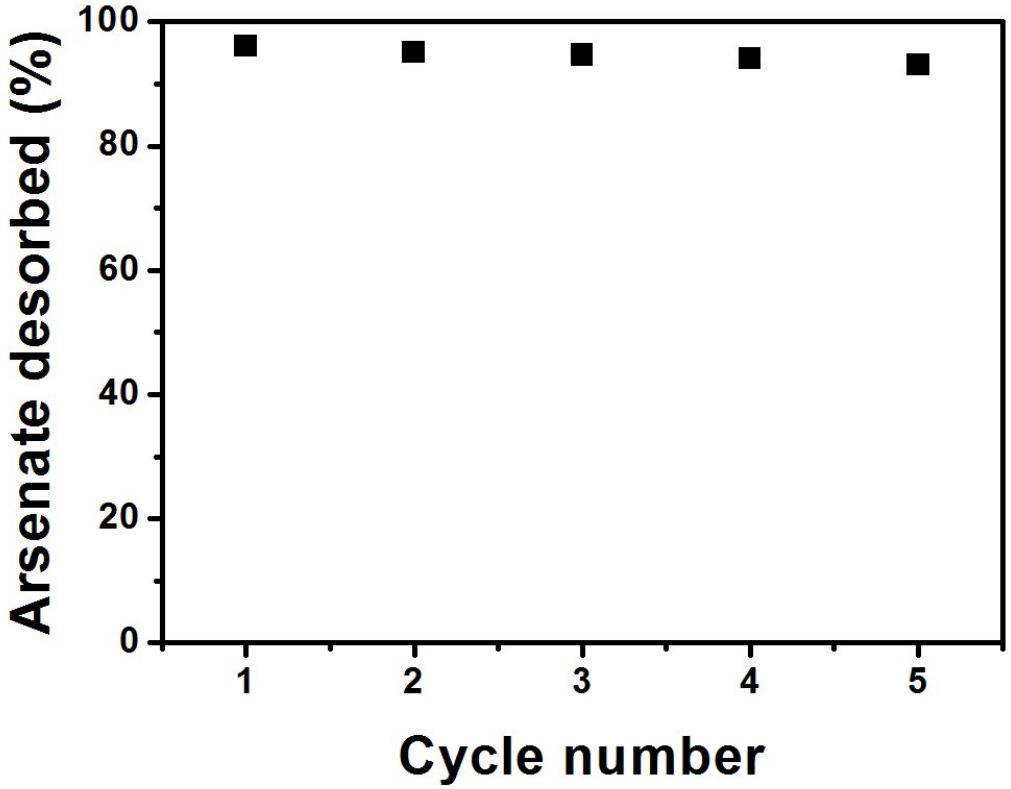

Fig. S9 The As^V desorption curves of the Fe_3O_4@RF@mTiO_2 microspheres. The desorption processes were conducted by using 0.5 M NaOH solution.

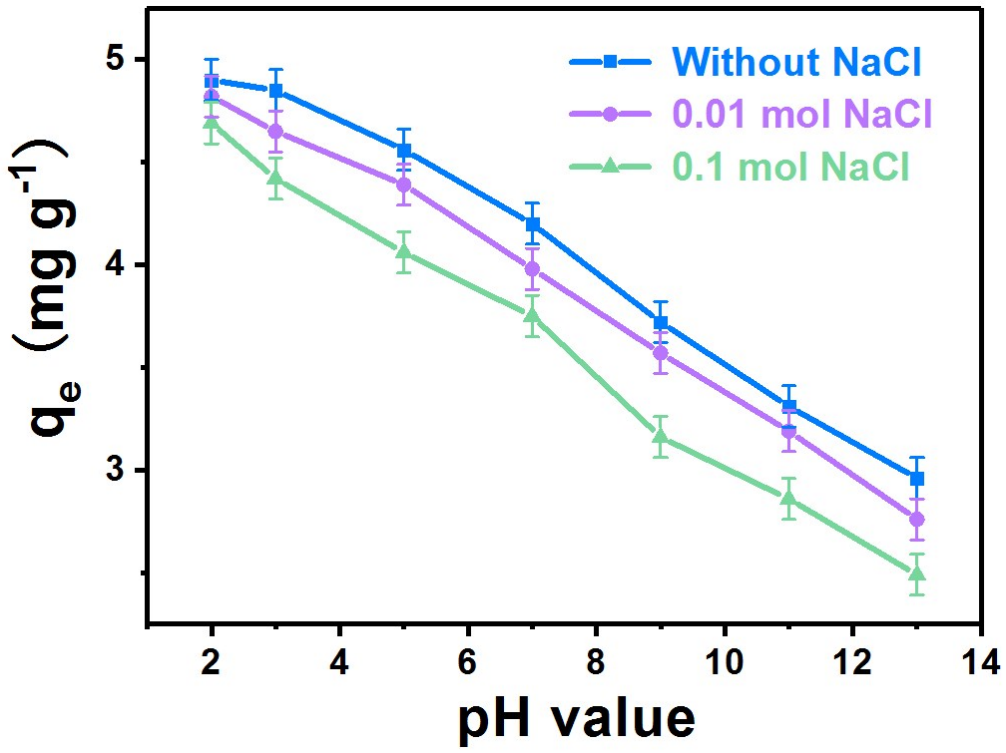

Fig. S10 Effect of ion strength on As^V adsorption by the multilayer Fe_3O_4@RF@mTiO_2 microspheres. The increased concentration of NaCl induces a competition effect with As^V removal, suggesting an electrostatic interaction between As^V and TiO_2 shells. The multilayer Fe_3O_4@RF@mTiO_2 microspheres were fabricated by calcining the as-made Fe_3O_4@RF@mTiO_2 microspheres at 200 °C for 3 h in air.

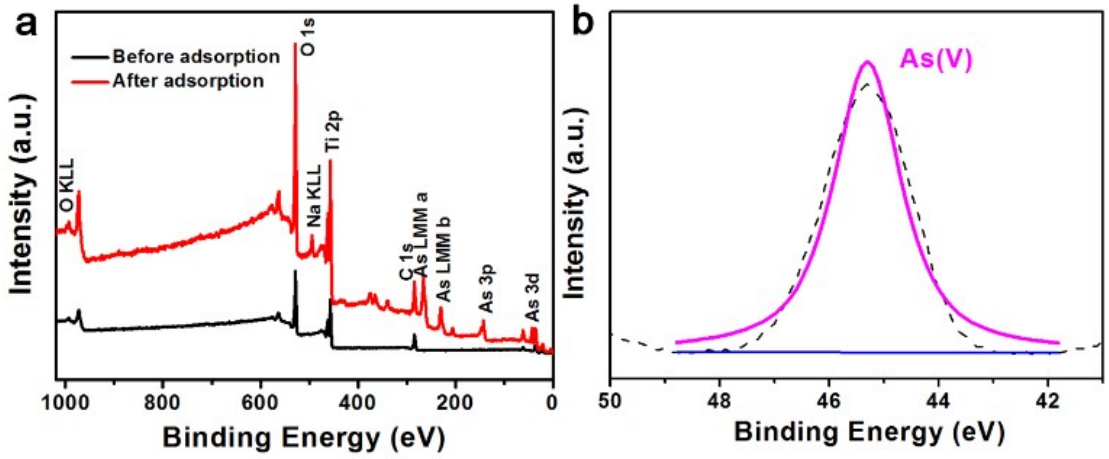

Fig. S11 (a) XPS wide scan spectra of the multilayer Fe_3O_4@RF@mTiO_2 microspheres before and after As^V adsorption. (b) High resolution As3d spectrum of the Fe_3O_4@RF@mTiO_2 microspheres after As^V adsorption, indicating the presence of As^V on the surface of the microspheres after adsorption. The multilayer Fe_3O_4@RF@mTiO_2 microspheres were fabricated by calcining the as-made Fe_3O_4@RF@mTiO_2 microspheres at 200 °C for 3 h in air.

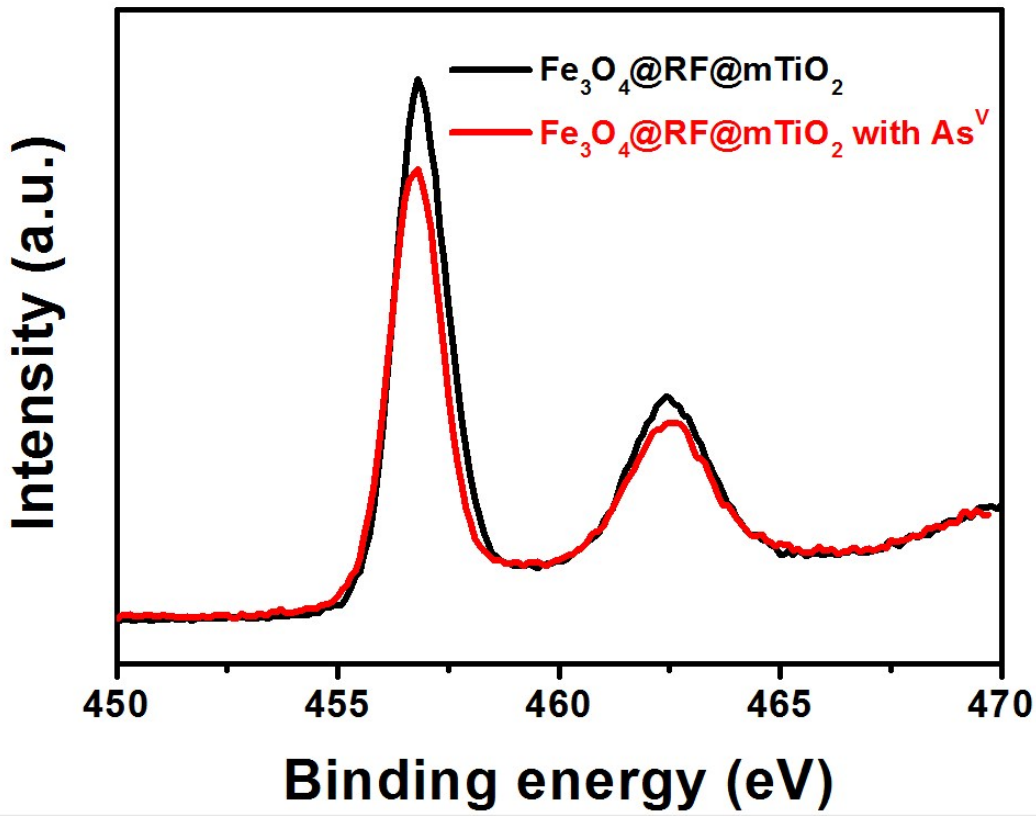

Fig. S12 Ti2p spectra of the multilayer Fe_3O_4@RF@$mTiO_2$ microspheres before and after arsenate adsorption. It can be found that the intensity of Ti2p bands slightly decreases after arsenate adsorption, which can be ascribed to the formation of surface coordination complex, thus shielding the surface exposure of Ti. The multilayer Fe_3O_4@RF@$mTiO_2$ microspheres were fabricated by calcining the as-made Fe_3O_4@RF@$mTiO_2$ microspheres at 200 °C for 3 h in air.

Table S1 Textural properties of the core-shell structured Fe_3O_4@RF@mTiO_2 and Fe_3O_4@mTiO_2 microspheres, their maximum adsorption capacities (q_{max}), and the rate constants of the pseudo-second-order model.

Samples	S_{BET} ($m^2 \cdot g^{-1}$)[a]	V_t ($cm^3 \cdot g^{-1}$)[b]	Pore size (nm)[c]	q_{max} ($mg \cdot g^{-1}$)[d]	R_1^2 [e]	k ($g \cdot mg^{-1} \cdot h^{-1}$)[f]	R_2^2 [g]
Fe_3O_4@RF@mTiO_2	337	0.38	3.0	138.6	0.997	1.16	0.999
Fe_3O_4@mTiO_2	351	0.42	2.7	143.2	0.996	1.37	0.999

[a], S_{BET} represents BET specific surface area obtained from N_2 adsorption data in the p/p_0 range from 0.05 to 0.20; [b], V_t represents the total pore volume calculated from the adsorbed amount at p/p_0 = 0.99; [c], Pore size is determined by using the Barrett-Joyner-Halenda (BJH) model. [d], q_{max} is the maximum adsorption capacity obtained by fitting with Langmuir model; [e], R_1^2 represents correlation coefficient related to the Langmuir mode; [f], k is the rate constant related to the pseudo-second-order rate mode; [g], R_2^2 represent correlation coefficient related to the pseudo–second–order rate mode.